RASĀYAN *J. Chem.*
Vol. 19 | No. 3 | 1228-1237 | July-September | 2026
ISSN: 0974-1496 | e-ISSN: 0976-0083 | CODEN: RJCABP
http://www.rasayanjournal.com
http://www.rasayanjournal.co.in

ENHANCED FILTRATION PERFORMANCE OF POLYAMIDE NANOFILTRATION MEMBRANES MODIFIED WITH POLYETHYLENE GLYCOL AND PRECIPITATED CALCIUM CARBONATE

B. Aritonang✉, A.H. Ritonga, H. Herlina, S. Samran, K. Harefa, and B. Irawan
Institut Kesehatan Medistra Lubuk Pakam, Deli Serdang-20512, (North Sumatra) Indonesia
✉Corresponding author: baritaaritonang11@gmail.com

ABSTRACT
Polyamide (PA) nanofiltration membranes are widely used in water treatment; however, their performance is often limited by insufficient hydrophilicity, permeability, and fouling resistance. This study aimed to enhance the filtration performance and physicochemical properties of PA membranes by incorporating polyethylene glycol (PEG) as a hydrophilic modifier and precipitated calcium carbonate (PCC) as an inorganic functional filler. The membranes were fabricated via a blending and phase-inversion method, with PEG content varying from 10–30 wt.% and PCC at 1–5 wt.% based on an optimized PA/PEG composition. The results showed that PEG significantly improved membrane hydrophilicity and permeability, with PWF reaching 60.0 L m^{-2} h^{-1} at the optimal PA/PEG ratio of 85/15 wt.%. Further PEG addition reduced permeability and salt rejection due to increased structural resistance. The incorporation of PCC further enhanced membrane performance, with the membrane containing 3 wt.% PCC achieving the highest PWF of 75.0 L m^{-2} h^{-1}, stable salt rejection, and superior antifouling performance, as indicated by a flux recovery ratio of 96.0% and an irreversible fouling ratio of 4.0%. Thermal and structural analyses confirmed that PEG and PCC did not alter the PA backbone, while effectively improving membrane permeability, fouling resistance, and operational durability. These findings highlight the potential of PEG and PCC modification as an effective strategy to overcome permeability-selectivity trade-offs and develop high-performance nanofiltration membranes for water treatment applications.
Keywords: Polyamide, PEG, PCC, Nanocomposite Membranes, Physicochemical Properties.
RASĀYAN *J. Chem.*, Vol. 19, No.3, 2026

INTRODUCTION

Polyamide (PA) membranes are widely used in nanofiltration because of their excellent chemical resistance, mechanical strength, and ability to form dense, selective layers, enabling efficient separation with low energy consumption. Consequently, PA membranes are extensively applied in water and wastewater treatment.[1,2] Their separation performance is governed by physicochemical properties such as membrane morphology, surface hydrophilicity, and thermal stability, which influence permeation, solute rejection, and fouling behavior.[3–5] However, the relatively hydrophobic nature of PA surfaces contributes to fouling, altering the membrane's physicochemical properties and reducing flux and lifespan.[6–9] Polymer blending with hydrophilic additives is a widely adopted strategy to tailor membrane physicochemical characteristics and improve filtration performance. Polyethylene glycol (PEG) is a hydrophilic, chemically stable polymer commonly used as a pore-forming and surface-modifying agent, and its effectiveness is reflected in changes in water flux, salt rejection, and fouling resistance.[10–12] The incorporation of inorganic fillers has been reported to further enhance the physicochemical properties of membranes.[13–16] Among various fillers, precipitated calcium carbonate (PCC), which possesses a controlled particle size and good dispersibility, has been reported to modify membrane morphology and thermal stability, thereby enhancing membrane durability during filtration operations.[17–19] Although the individual effects of PEG and PCC on PA membranes have been reported,[10,11] a comprehensive understanding of their combined effect on both filtration performance and physicochemical properties remains limited, particularly in establishing a clear correlation between membrane structure, permeability,

http://doi.org/10.31788/RJC.2026.1939755

selectivity, and fouling behavior. This limitation highlights the need for a systematic approach to optimize membrane performance while maintaining structural stability and durability. Accordingly, this study aims to evaluate the filtration performance of PA nanofiltration membranes modified with PEG and PCC, followed by physicochemical characterization to elucidate the relationship between membrane structure and performance. Furthermore, this work contributes to Sustainable Development Goal (SDG) 6 (Clean Water and Sanitation) by proposing an effective strategy for developing high-performance nanofiltration membranes for improved water treatment applications.

EXPERIMENTAL

Material

Polyamide-6 (PA6) was purchased from Sigma-Aldrich (USA). Polyethylene Glycol 400 (PEG 400) and Precipitated Calcium Carbonate (PCC) were supplied by Merck (Germany). Bovine Serum Albumin (BSA) and phosphate buffer solution (pH 7.0) were purchased from Sigma-Aldrich (USA). Hydrochloric acid (HCl, 25%) and sodium chloride (NaCl) were obtained from Merck (Germany). Deionized water was supplied by OneMed (Indonesia).

Modification of PA Nanofiltration Membranes with PEG

PA was weighed according to the compositions listed in Table-1 and dissolved in 100 mL of 25% HCl under continuous stirring (500 rpm at 25 ± 2°C) until a homogeneous solution was obtained. PEG was then added at various concentrations, followed by further stirring (500 rpm for 2 h) to form a uniform polymer dope solution. The prepared dope solution was allowed to stand for 24 h (at room temperature, 25 ± 2°C) to remove entrapped air bubbles. The dope solution was cast onto a clean glass plate and spread uniformly using a casting knife (with a controlled thickness of 150 μm) to obtain a thin film. The cast film was left for 10 min (under ambient conditions) to allow partial solvent evaporation, then immersed in a coagulation bath containing deionized water (25 ± 2°C) to induce phase inversion. The resulting membranes were thoroughly rinsed and dried at room temperature (25 ± 2°C) for 24 h.

Modification of PA Nanofiltration Membranes with PEG and PCC

For the preparation of the AEC series, PA was weighed according to the formulation shown in Table-1 and dissolved in 100 mL of 25% HCl under continuous stirring (500 rpm at 25±2°C) until a homogeneous solution was obtained. PEG was then added at a fixed concentration, followed by the incorporation of PCC at different loadings. The mixture was stirred continuously (500 rpm for 2 h) to ensure uniform dispersion of the inorganic filler within the polymer matrix. The resulting dope solution was degassed for 24 h (at 25 ± 2°C) before casting. Membrane casting and phase inversion were performed using the same procedure described in the previous section. After complete detachment, the composite membranes were washed thoroughly with deionized water and dried at room temperature (at 25 ± 2 °C) for 24 h. The selected PEG and PCC compositions were based on preliminary optimization to obtain balanced permeability, selectivity, and antifouling performance.

Table-1: Composition of PA/PEG and PA/PEG/PCC Nanofiltration Membranes

Sample Code		PA (wt.%)	PEG (wt.%)	Sample Code		PA (wt.%)	PEG (wt.%)	PCC (wt.%)
PA/PEG (AE series)	AE0	100	0	PA/PEG/PCC (AEC series)	AEC-0	85	15	0
	AE1	90	10		AEC-1	85	14	1
	AE2	85	15		AEC-2	85	13	2
	AE3	80	20		AEC-3	85	12	3
	AE4	75	25		AEC-4	85	11	4
	AE5	70	30		AEC-5	85	10	5

Pure Water Flux and Water Permeability Measurements

Pure water flux (PWF) and water permeability (WP) were measured using a stirred dead-end filtration cell operated at a constant transmembrane pressure of 10 bar. The membrane was placed in the filtration cell with the active layer facing the feed side, and deionized water at 25±1 °C was used as the feed

solution. Prior to data collection, the membrane was compacted at the operating pressure for 30-60 min until a stable flux was achieved (flux variation < 5%), and the permeate obtained during this compaction stage was discarded. After stabilization, permeate was collected at 5-10 min intervals, and its volume was measured; the experiment was repeated at least three times (n = 3). The obtained PWF data were subsequently used to calculate the WP. The PWF and WP were calculated using the following equations:

$$J = \frac{V}{(A.t)} \ , \ L_p = \frac{J}{\Delta P}$$

Where: J = pure water flux (L/m² h), V = permeate volume (L), A = effective membrane area (m²), t = filtration time (h), L_p = water permeability (L/m² h bar), and ΔP = the applied pressure (bar).

Salt Rejection Evaluation

Salt rejection was evaluated using a 1000 mg/L NaCl solution. The membrane was installed in the filtration cell with the active layer facing the feed side and pre-compressed at an operating pressure of 10 bar until the flux variation was less than 5%. After stabilization, filtration was performed at 10 bar and 25 ±1°C under steady-state conditions. Feed and permeate samples were collected, and the salt concentrations in the feed (C_f) and permeate (C_p) were determined based on conductivity measurements (using a calibrated conductivity meter). Salt rejection (R) was calculated using the following equation:

$$R(\%) = \left(1 - \frac{C_p}{C_f}\right) \times 100$$

Where: C_p = salt concentration in permeate (mg/L), and C_f = salt concentration in feed (mg/L).

Fouling Test

The fouling test was conducted after measuring the initial pure water flux (J_0). The feed solution was then replaced with a BSA solution (1 g/L at pH 7), and filtration was performed at 10 bar for 60–120 min (until steady-state flux decline was observed). During this stage, the permeate flux (J_t) was recorded until the final fouling flux (J_f) was obtained. After fouling, the membrane was physically cleaned by flushing with deionized water at low pressure for 10–15 min, after which the pure water flux after cleaning (J_r) was measured. The fouling behavior was evaluated based on flux recovery ratio (FRR), total fouling ratio (R_t), reversible fouling ratio (R_{rev}), and irreversible fouling ratio (R_{irrev}), calculated using the following equations:

$$FRR(\%) = \left(\frac{J_r}{J_0}\right) \times 100 \ , \quad R_t(\%) = \left(1 - \frac{J_f}{J_0}\right) \times 100,$$

$$R_{rev}(\%) = \frac{J_r - J_f}{J_0} \times 100, \quad R_{irrev}(\%) = \frac{J_0 - J_r}{J_0} \times 100$$

where: J_0 = initial pure water flux (L/m² h), J_f = final fouling flux (L/m² h), and J_r = flux after physical cleaning (L/m² h).

Characterization

Thermal stability and degradation behavior of the membranes were evaluated using thermogravimetric and differential thermal analysis (TGA/DTA; Hitachi STA-7300) under a nitrogen atmosphere (flow rate ~50 mL/min) at a heating rate of 10 °C min^{-1}. Chemical functional groups were identified by Fourier-transform infrared spectroscopy (FTIR; Agilent Cary 630) over the wavenumber range of 4000–650 cm^{-1} (resolution 4 cm^{-1}). The surface morphology of the samples was examined using scanning electron microscopy (SEM, ZEISS EVO MA-10) at an accelerating voltage of 5–10 kV after gold sputter coating.

RESULTS AND DISCUSSION

Pure Water Flux and Water Permeability Behavior

The pure water flux (PWF) and water permeability (WP) of the PA/PEG (AE series) and PA/PEG/PCC (AEC series) nanofiltration membranes are presented in Fig.-1. In the AE series, the incorporation of PEG into the PA matrix resulted in a significant enhancement of both PWF and WP compared with the control membrane (AE-0). The performance increased with PEG content and reached an optimum at AE-2,

indicating that PEG effectively improved membrane hydrophilicity and facilitated water transport at moderate loading. However, further addition of PEG (AE-3 to AE-5) led to a decline in both parameters, suggesting that excessive PEG adversely affected water transport, likely due to increased structural resistance, as reported in previous studies.[20–22] Therefore, AE-2 was identified as the optimum composition within the PA/PEG membrane series. For the AEC series, incorporating PCC into the optimized PA/PEG matrix (AE-2) further improved both PWF and WP. The membrane performance increased with PCC loading and reached a maximum at AEC-3, confirming the beneficial role of PCC as a hydrophilic inorganic filler that enhances water transport. At higher PCC contents (AEC-4 and AEC-5), performance decreased, indicating that excessive PCC loading negatively affected membrane structure and transport pathways. Similar trends have been reported for $CaCO_3$-filled polymeric membranes.[23–25] Accordingly, AEC-3 was determined to be the optimum composition for the PA/PEG/PCC membrane system. This result indicates an effective balance between permeability and membrane structure, contributing to improved nanofiltration performance for water treatment applications (SDG 6).

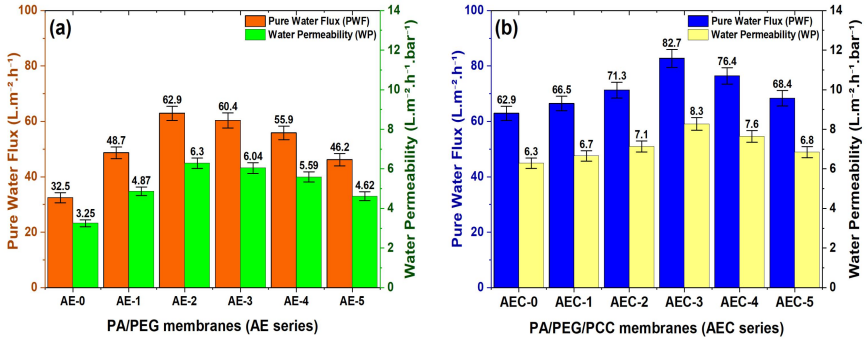

Fig.-1: The PWF and WP of (a) PA/PEG Membranes and (b) PA/PEG/PCC Membranes

Salt Rejection Performance

The salt rejection characteristics of the PA/PEG (AE) nanofiltration membranes are illustrated in Fig.-2a. Within this series, salt rejection exhibited a gradual decline as the PEG content increased. While the pristine membrane (AE-0) maintained the highest rejection levels, the addition of PEG enhanced membrane hydrophilicity and flexibility. This modification likely increased the effective pore size and, consequently, reduced selectivity, a phenomenon consistent with previous studies.[4, 13,25]

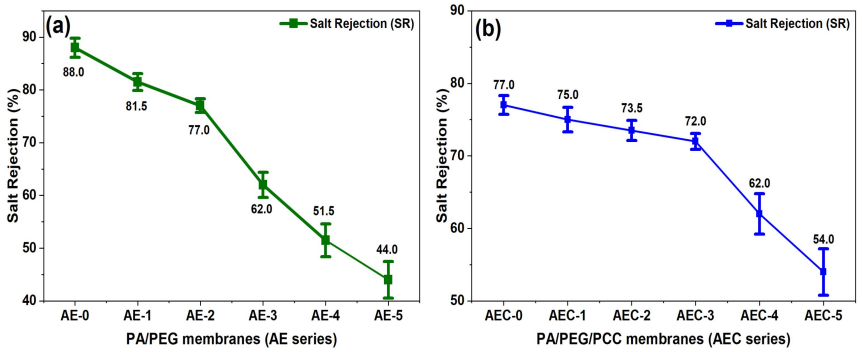

Fig.-2: The Salt Rejection of (a) PA/PEG Membranes and (b) PA/PEG/PCC Membranes

Among the AE group, AE-2 emerged as the formulation with the most balanced performance in terms of salt rejection and permeability. Regarding the PA/PEG/PCC (AEC) membranes, the salt rejection data are presented in Fig.-2b. The incorporation of PCC yielded higher, more stable rejection rates than the AE series at equivalent compositions. It appears that moderate PCC loading helps maintain membrane selectivity by improving structural stability and pore regulation.[16,26] However, exceeding the optimal PCC content led to reduced salt rejection, presumably due to particle agglomeration and the formation of non-selective transport pathways.[27,28] Consequently, AEC-3 was identified as the optimum composition, offering the best compromise between salt rejection and overall filtration efficiency. This finding

demonstrates the ability to reduce the permeability–selectivity trade-off, which is a key challenge in membrane development.

Fouling Performance

The fouling performance of AE and AEC membranes evaluated using a 1 g/L BSA solution is presented in Table-2. In the AE series, increasing PEG content improved antifouling properties, with AE2 at the optimum condition exhibiting the highest flux recovery ratio (FRR) of 90.0% and a low irreversible fouling ratio (R_{irrev}) of 10.0%. This indicates that PEG at an optimal concentration enhances membrane hydrophilicity and reduces protein adsorption, as reported in previous studies.[28,29] Further PEG addition did not result in significant improvement, likely due to structural heterogeneity or pore blockage.[30,31] The incorporation of PCC in the AEC series markedly enhanced membrane fouling resistance. AEC0 showed fouling behavior identical to that of AE2, confirming AE2 as the baseline membrane. Among the AEC membranes, AEC3 demonstrated the best performance, with the highest FRR (96.0%) and the lowest R_{irrev} (4.0%), indicating that PCC acts as a functional filler that suppresses strong protein–membrane interactions by increasing surface hydrophilicity.[22,29] The dominance of reversible fouling in AEC membranes suggests that foulants can be readily removed by physical cleaning, which is advantageous for long-term nanofiltration applications.[25,32] This improvement enhances membrane durability and supports its practical application in sustainable water treatment systems.

Table-2: Fouling Performance of AE and AEC Membranes Using BSA Solution

Sample		J_0 (L/m² h)	J_f (L/m² h)	J_r (L/m² h)	FRR (%)	Rt (%)	R_{rev} (%)	R_{irrev} (%)
AE series	AE0	45.0 ± 2.1	20.3 ± 1.0	30.6 ± 1.4	68.0	54.9	22.9	32.0
	AE1	50.0 ± 2.3	28.0 ± 1.3	35.0 ± 1.6	70.0	44.0	14.0	30.0
	AE2	60.0 ± 2.8	42.0 ± 1.9	54.0 ± 2.2	90.0	30.0	20.0	10.0
	AE3	68.0 ± 3.0	44.9 ± 2.1	58.5 ± 2.4	86.0	34.0	20.0	14.0
	AE4	75.0 ± 3.4	53.3 ± 2.5	66.8 ± 2.9	89.1	28.9	18.0	10.9
	AE5	82.0 ± 3.6	60.7 ± 2.8	74.6 ± 3.1	91.0	26.0	17.0	9.0
AEC series	AEC0	60.0 ± 2.8	42.0 ± 1.9	54.0 ± 2.2	90.0	30.0	20.0	10.0
	AEC1	65.0 ± 3.0	46.8 ± 2.2	59.8 ± 2.6	92.0	28.0	20.0	8.0
	AEC2	70.0 ± 3.2	52.5 ± 2.4	64.4 ± 2.9	92.0	25.0	17.0	8.0
	AEC3	75.0 ± 3.5	60.0 ± 2.7	72.0 ± 3.1	96.0	20.0	16.0	4.0
	AEC4	80.0 ± 3.7	62.4 ± 2.9	75.2 ± 3.3	94.0	22.0	16.0	6.0
	AEC5	85.0 ± 3.9	65.5 ± 3.1	79.1 ± 3.5	93.0	23.0	14.0	7.0

Thermal Analysis

Figure-3 shows the TGA, DTG, and DTA curves of PA, PA/PEG (AE), and PA/PEG/PCC (AEC) membranes, with the thermal parameters summarized in Table-3. All samples exhibit similar $T_{1\%}$ values (27.5–27.7 °C), indicating comparable initial mass loss related to moisture and volatile components. The addition of PEG increases $T_{5\%}$ from 44.5°C to 89.0°C, suggesting a delay in early-stage mass loss. This trend is consistent with previous studies showing that PEG can improve low-temperature thermal resistance in polyamide systems by enhancing intermolecular interactions.[14,33] In contrast, the $T_{5\%}$ value of AEC decreases to a level close to that of neat PA, suggesting that PCC weakens PEG's stabilizing effect at low temperatures. DTG analysis shows that AE exhibits nearly identical T_{max} values (~450 °C), confirming that PEG does not significantly affect the main degradation temperature of PA, in agreement with earlier reports on PEG-modified polyamides.[34,35] However, incorporating PCC results in a pronounced decrease in T_{max} to 391.5 °C. Similar reductions have been reported for $CaCO_3$-filled polymer systems, where $CaCO_3$ acts as a functional filler that modifies degradation pathways rather than enhancing thermal stability.[19,36] DTA results show a gradual decrease in melting temperature (T_m) and decomposition temperature (T_d) with the addition of PEG and PCC. This behavior has also been observed in previous studies, where mineral fillers disrupt polymer crystallinity and introduce a trade-off in high-temperature stability.[33,37] Overall, PEG modifies the early thermal behavior of PA without altering the main degradation temperature, whereas PCC alters melting and degradation as a functional filler.[10,28] These results confirm that performance enhancement is achieved without compromising thermal stability.

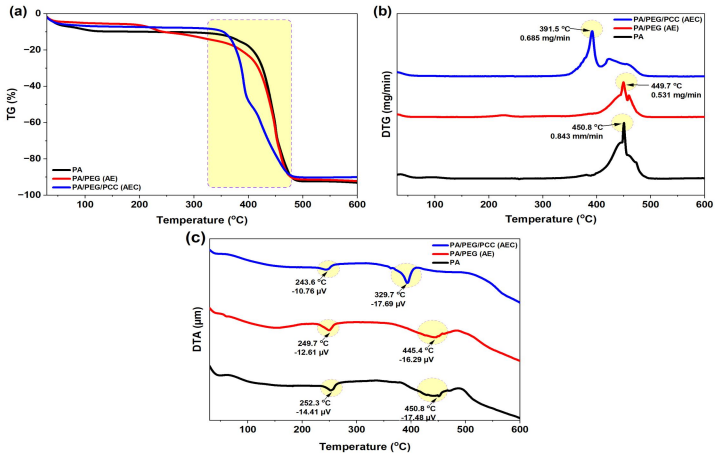

Fig.-3: (a) TGA, (b) DTG, and (c) DTA of PA, AE, and AEC

Table-3: Thermal properties of PA, PA/PEG (AE), and PA/PEG/PCC (AEC)

Sample	$T_{1\%}$ (°C)	$T_{5\%}$ (°C)	T_{max} (°C)	T_m (°C)	T_d (°C)
PA	27.5	44.5	450.8	252.3	450.8
PA/PEG (AE)	27.6	89.0	449.7	249.7	445.5
PA/PEG/PCC (AEC)	27.7	46.0	391.5	243.6	329.7

Note: $T_{1\%}$ = temperature at 1% weight loss; $T_{5\%}$ = temperature at 5% weight loss; T_{max} = temperature of maximum degradation rate (DTG); T_m = melting temperature (DTA); T_d = decomposition temperature (DTA).

Chemical Functional Group Analysis

The FTIR spectra of PA, AE, and AEC membranes exhibit the characteristic absorption bands of polyamide (Fig.-4), including broad N–H stretching vibrations in 3302.4 cm^{-1}, C–H stretching bands in the 2937.1–2862.5 cm^{-1} region, and the amide I band (1632.5 cm^{-1}), mainly associated with C=O stretching, and the amide II band (1535.6 cm^{-1}), attributed to C–N stretching coupled with N–H bending. These bands are consistent with previously reported FTIR results for PA/$CaCO_3$ composites, which confirmed that the fundamental PA backbone remains intact after filler addition.[10,38] Compared with neat PA, the AE membrane shows increased intensity in the C–H stretching region, attributable to the –CH_2 groups of the PEG. The absence of new absorption bands or significant peak shifts suggests that PEG interacts with the PA matrix primarily through physical interactions, such as hydrogen bonding, rather than by forming new covalent bonds. Similar observations have been reported in PEG-modified polymer blends, where PEG incorporation does not change the main spectral features of the polymer but modifies the relative intensities of existing bands.[10,39]

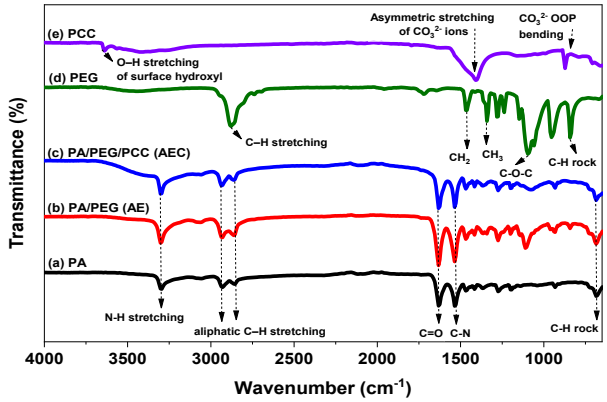

Fig.-4: FTIR Spectra of (a) PA, (b) PA/PEG (AE), (c) PA/PEG/PCC (AEC), (d) PEG, and (e) PCC

In the AEC membrane, additional absorption features are observed near 1416.3–1468.5 cm^{-1} and around 842.3 cm^{-1}, corresponding to typical carbonate (CO_3^{2-}) vibrational modes of calcium carbonate, which are

well documented in FTIR analyses of $CaCO_3$-based materials. The appearance of these carbonate bands confirms the successful incorporation of PCC into the composite.[14, 30,40] The FTIR analysis indicates that the incorporation of PEG and PCC does not alter the characteristic absorption features of the polyamide backbone.[8,9] The presence of PEG and PCC is reflected primarily in changes in band intensities and the emergence of additional absorption bands associated with each component. In this system, PEG serves as a polymer modifier, while PCC functions as a functional filler, in agreement with previous reports on polyamide/$CaCO_3$ composites. This indicates that the performance improvement is mainly due to structural modification rather than chemical changes.

Morphological Analysis

The surface morphologies of PA, AE, and AEC membranes at magnifications of 1000× and 10,000× are shown in Fig.-5. Neat PA (a,d) exhibits a relatively smooth and homogeneous fracture surface, which is characteristic of brittle failure behavior commonly reported for unmodified PA due to its limited chain mobility.[41] After the incorporation of PEG, the AE membrane (b,e) shows a noticeably rougher surface morphology compared to neat PA. The appearance of shallow grooves and micro-scale irregularities indicates enhanced ductility and increased polymer chain mobility induced by PEG. Similar SEM features have been reported in PEG-modified PA systems, where PEG acts as a plasticizing modifier and promotes more energy-dissipative fracture behavior without causing phase separation.[3,7,42] For the AEC membrane (c,f), the surface morphology becomes more heterogeneous. At lower magnification (c), the presence of dispersed PCC particles contributes to a less uniform surface, while higher magnification images (f) reveal PCC particles embedded within the polymer matrix. The particles appear relatively well distributed with no large voids or severe agglomeration, suggesting acceptable interfacial contact between PCC and the PA/PEG matrix. This morphology is consistent with previous studies on $CaCO_3$-filled polymer composites, in which PCC acts as a functional filler that modifies fracture topography primarily through physical and interfacial interactions rather than chemical bonding.[8,29,43] Overall, the SEM observations indicate that PEG primarily modifies the matrix morphology by enhancing ductility and matrix continuity, whereas PCC introduces microstructural heterogeneity associated with filler incorporation. These microstructural characteristics support the role of PEG as a polymer modifier and PCC as a functional filler in the PA-based composite system. This structure–performance relationship explains the observed improvement in filtration performance.

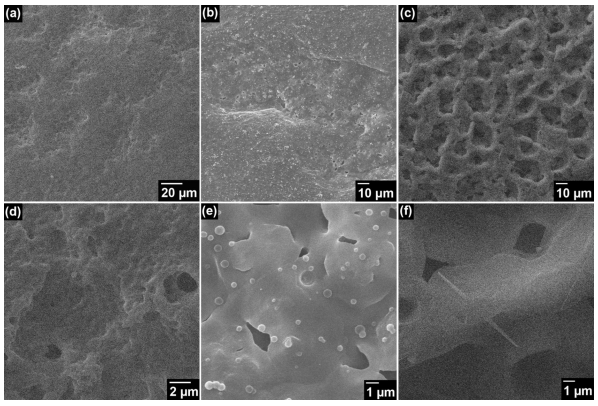

Fig.-5: SEM Micrographs of (a, d) PA, (b, e) PA/PEG (AE), and (c, f) PA/PEG/PCC (AEC) Showing the Surface Morphology at 1000× (a–c) and 10,000× (d–f) Magnifications

CONCLUSION

PA nanofiltration membranes were modified with PEG and PCC to improve filtration performance. The incorporation of PEG enhanced membrane hydrophilicity and water permeability, with optimal performance achieved at a PA/PEG ratio of 85/15 wt.%, while excessive PEG reduced permeability and salt rejection. The addition of PCC further improved permeability, salt rejection stability, and fouling resistance, with the best performance obtained at 3 wt.% PCC. Fouling analysis indicated predominantly reversible fouling, and thermal, FTIR, and SEM results confirmed that PEG- and PCC-modified

membranes retained PA backbone properties. Overall, the combined use of PEG and PCC provides a balanced enhancement in permeability, selectivity, and membrane stability, representing an effective strategy for improving nanofiltration membrane performance. These findings demonstrate the potential application of the developed membranes in water treatment systems, supporting Sustainable Development Goal (SDG) 6: Clean Water and Sanitation. Furthermore, future studies are recommended to investigate long-term operational stability and scale-up feasibility for practical applications.

ACKNOWLEDGMENTS

The author gratefully acknowledges the Directorate of Research and Community Service, Directorate General of Research and Development, Ministry of Higher Education, Science, and Technology of the Republic of Indonesia, for financial support through the Fundamental Research Grant under Decree No. 0070/C3/AL.04/2025 dated 23 May 2025, including the implementation of the Main Research Contract No. 122/C3/DT.05.00/PL/2025 and the Derivative Contracts No. 49/SPK/LL1/AL.04.03/PL/2025 and No. 016/AK/LPPM/INKES-MLP/VI/2025.

CONFLICT OF INTERESTS

The authors declare that there is no conflict of interest.

AUTHOR CONTRIBUTIONS

The present work is related to *SDG-6: Clean Water and Sanitation.* All the authors contributed significantly to this manuscript, participated in reviewing/editing and approved the final draft for publication. The research profile of the authors can be verified from their ORCID ids, given below:

B. Aritonang https://orcid.org/0000-0003-0699-1768
A.H. Ritonga https://orcid.org/0000-0002-8415-5549
H. Herlina https://orcid.org/0000-0002-4966-8592
S. Samran https://orcid.org/0000-0002-6214-4523
K. Harefa https://orcid.org/0000-0002-4661-9656
B. Irawan https://orcid.org/0000-0003-0608-5562

Cite this article as: B. Aritonang *et al.*, *Rasayan J. Chem.*, 19(3), 1228-1237(2026), https://doi.org/10.31788/RJC.2026.1939755

REFERENCES

1. M. A. Akram, S. Zhao, M. Wang, M. Hussain, and Q. J. Niu, *Desalination*, **620,** 119677(2026), https://doi.org/10.1016/j.desal.2025.119677
2. B. Aritonang, Tamrin, B. Wirjosentono, and Eddiyanto, *Case Studies in Thermal Engineering*, **21,** 100690(2020), https://doi.org/10.1016/j.csite.2020.100690
3. A. Ahamad, G. Tiwari, D. Singh, R. Kumar, and S. Patil, *Journal of the Indian Chemical Society*, **103,** 102362(2026), https://doi.org/10.1016/j.jics.2025.102362
4. B. M. Jun, Y. K. Kim, and Y. N. Kwon, *Desalination*, **614,** 119120(2025), https://doi.org/10.1016/j.desal.2025.119120
5. Y. R. Zhu, H. Tang, H.-R. Zuo, and M. Duan, *Journal of Membrane Science*, **728,** 124136(2025), https://doi.org/10.1016/j.memsci.2025.124136
6. S. Hao, L. Liu, J. Xiao, J. Wang, Y. Xu, and Y. Hu, *Journal of Membrane Science*, **707,** 122994(2024), https://doi.org/10.1016/j.memsci.2024.122994
7. J. Kidd, D. Hatinoglu, K. Mensah, L. Ochoa, K. Nguyen, B. Yan, N. Fahrenfeld, O. Apul, and P. Stapleton, *Science of The Total Environment*, **1012,** 181214(2026), https://doi.org/10.1016/j.scitotenv.2025.181214
8. R. Li, M. He, S. Han, L. Li, P. Chen, X. Wang, Y. Tong, J. Gong, H. Wang, Y. Zhang, and J. Zhu,

Desalination, **616**, 119334(2025), https://doi.org/10.1016/j.desal.2025.119334
9. S. S. Panchal, D. V Vasava, and R. Joshi, *Rasayan Journal of Chemistry*, **17,** 317(2024), https://doi.org/10.31788/RJC.2024.1728742
10. P. Khanalilou, L. Naji, S. Mehdipour-Ataei, and M. Abdouss, *Journal of Environmental Chemical Engineering*, **12,** 113748(2024), https://doi.org/10.1016/j.jece.2024.113748
11. M. B. M. Y. Ang, J. A. D. Marquez, C. C. Lin, H. L. Yang, Y.-S. Wang, S.-H. Huang, H.-A. Tsai, and K.-R. Lee, *Journal of the Taiwan Institute of Chemical Engineers*, **131,** 104157(2022), https://doi.org/10.1016/j.jtice.2021.11.024
12. Y. Rilda, F. Rivaldo, R. Admi, A. Armaini, and H. Pardi, *Rasayan Journal of Chemistry*, **16(2),** 714(2023), https://doi.org/10.31788/RJC.2023.1628232.
13. J. Joseph, Y.-A. Boussouga, M. Di Vincenzo, M. Barboiu, and A. I. Schäfer, *Journal of Membrane Science*, **664,** 121019(2022), https://doi.org/10.1016/j.memsci.2022.121019
14. D. Chen, X. Qin, X. Cao, N. Wang, and Y. Zhu, *Chemical Engineering Journal*, **450,** 137644(2022), https://doi.org/10.1016/j.cej.2022.137644
15. D. Chen, X. Qin, X. Cao, F. Wei, K. Thummavichai, O. Ola, N. Wang, M. Jiang, and Y. Zhu, *Journal of Cleaner Production*, **401,** 136630(2023), https://doi.org/10.1016/j.jclepro.2023.136630
16. Y. Liu, Y. Chen, H. Ding, J. Xue, Y. Yang, and X. Li, *Journal of Membrane Science*, **716,** 123525(2025), https://doi.org/10.1016/j.memsci.2024.123525
17. A. H. Ritonga, N. Jamarun, S. Arief, H. Aziz, D. A. Tanjung, and B. Isfa, *Rasayan Journal of Chemistry*, **15,** 190(2022), https://doi.org/10.31788/RJC.2022.1516720
18. A. H. Ritonga, N. Jamarun, S. Arief, H. Aziz, D. A. Tanjung, B. Isfa, V. Sisca, and H. Faisal, *Journal of Materials Research and Technology*, **17,** 2326(2022), https://doi.org/10.1016/j.jmrt.2022.01.125
19. B. Isfa, N. Jamarun, Emriadi, A. H. Ritonga, V. Sisca, H. Faisal, and D. A. Tanjung, *Rasayan Journal of Chemistry*, **15,** 2342(2022), https://doi.org/10.31788/RJC.2022.1547053
20. H. Zhou, Z. Qiu, J. Zeng, R. Dai, and Z. Wang, *Journal of Membrane Science*, **688,** 122125(2023), https://doi.org/10.1016/j.memsci.2023.122125
21. N. AL-Hamdani, G. Costanzo, G. Purpura, J. Luque Di Salvo, and G. De Luca, *Journal of Membrane Science*, **742,** 125128(2026), https://doi.org/10.1016/j.memsci.2026.125128
22. J. Ding, X. Ding, C. Wu, Y. Wu, and S. Xia, *Desalination*, **573,** 117188(2024), https://doi.org/10.1016/j.desal.2023.117188
23. H. Jiang, N. Yang, Y. Hao, L. Zhang, X. Xiao, Y. Sun, B. Jiang, and L. Zhang, *Separation and Purification Technology*, **347,** 127590(2024), https://doi.org/10.1016/j.seppur.2024.127590
24. X. Guo, B. Zhao, X. Di, L. Wang, and Z. Zhang, *Separation and Purification Technology*, **382,** 136035(2026), https://doi.org/10.1016/j.seppur.2025.136035
25. V. Kumar, N. Pandey, and J. Bellare, *Chemical Engineering Journal*, **527,** 171944(2026), https://doi.org/10.1016/j.cej.2025.171944
26. Y. Wu, C. Yao, Y. Wang, M. Ding, H. Xu, X. Yan, and L. Gao, *Journal of Environmental Chemical Engineering*, **12,** 111963(2024), https://doi.org/10.1016/j.jece.2024.111963
27. B. Zhang, W. Zou, P. Wu, J. Zhang, W. Kong, X. Chen, C. Wu, and Y. Wang, *Sustainable Materials and Technologies*, **40,** e00910(2024), https://doi.org/10.1016/j.susmat.2024.e00910
28. L. Wang, H. Yang, H. Li, P. Lu, Y. Yu, X. Zhang, Y. Wang, J. Xia, D. He, and Y. Li, *Desalination*, **549,** 116307(2023), https://doi.org/10.1016/j.desal.2022.116307
29. T. K. Arsene, Z. Zhai, J. Zhu, M. Tian, and Y. Zhang, *Desalination*, **603,** 118685(2025), https://doi.org/10.1016/j.desal.2025.118685
30. W. Zhang, G.-L. Ji, J. Wang, Y. He, L. Liu, and F. Liu, *Journal of Membrane Science*, **658,** 120713(2022), https://doi.org/10.1016/j.memsci.2022.120713
31. A. Harmes, A. C. Ambarita, N. Arahman, and S. Mulyati, *South African Journal of Chemical Engineering*, **48,** 237(2024), https://doi.org/10.1016/j.sajce.2024.02.008
32. D. J. Park, O. D. Supekar, A. R. Greenberg, J. T. Gopinath, and V. M. Bright, *Desalination and Water Treatment*, **273,** 92(2022), https://doi.org/10.5004/dwt.2022.28883

33. R. Zhao, R. Zhu, C. Li, Y. Yang, J. Yu, and X. Wang, *Polymer Degradation and Stability*, **242,** 111710(2025), https://doi.org/10.1016/j.polymdegradstab.2025.111710
34. J. Tanks, T. Akagawa, K. Tamura, Y. Nemoto, K. Naito, Y. Watanabe, T. T. Nge, and T. Yamada, *Polymer*, **335,** 128853(2025), https://doi.org/10.1016/j.polymer.2025.128853
35. W. L. Li, J. H. Xin, P. Fu, W. T. Lin, Z. L. Zhang, X. W. Luo, Z. K. Xu, and L. S. Wan, *Journal of Colloid and Interface Science*, **700,** 138509(2025), https://doi.org/10.1016/j.jcis.2025.138509
36. N. R. Sarker, P. Cherukupally, I. Gourevich, J. Wilbur, S. D. Jons, and A. M. Bilton, *Desalination*, **539,** 115956(2022), https://doi.org/10.1016/j.desal.2022.115956
37. S. A. Ravichandran, J. Hutfles, J. Velasco, J. Killgore, and J. Pellegrino, *Colloids and Surfaces A: Physicochemical and Engineering Aspects*, **619,** 126473(2021), https://doi.org/10.1016/j.colsurfa.2021.126473
38. A. H. Ritonga, V. Sisca, B. Aritonang, D. Meilani, G. E. Putri, and E. W. B. Siahaan, *South African Journal of Chemical Engineering*, **52**, 1(2025), https://doi.org/10.1016/j.sajce.2025.01.005
39. F. G. de A. Dias, A. G. Veiga, A. P. A. da C. P. Gomes, M. F. da Costa, and M. L. M. Rocco, *Polymer Degradation and Stability*, **195,** 109787(2022), https://doi.org/10.1016/j.polymdegradstab.2021.109787
40. A. H. Ritonga, B. Aritonang, G. E. Putri, K. Khairiah, E. W. B. Siahaan, and D. Meilani, *Indonesian Journal of Chemistry*, **23,** 1694(2023), https://doi.org/10.22146/ijc.86983
41. A. El-Gendi, *Desalination and Water Treatment*, **255,** 120(2022), https://doi.org/10.5004/dwt.2022.28333
42. Z. Ju, N. Brosse, S. Hoppe, Z. Wang, I. Ziegler-Devin, H. Zhang, and B. Shu, *International Journal of Biological Macromolecules*, **262**, 129997(2024), https://doi.org/10.1016/j.ijbiomac.2024.129997
43. T. Suzuki, R. Tanaka, M. Tahara, Y. Isamu, M. Niinae, L. Lin, J. Wang, J. Luh, and O. Coronell, *Water Research*, **100,** 326(2016), https://doi.org/10.1016/j.watres.2016.04.068

[RJC-9755/2026]